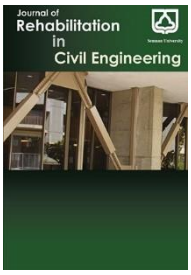

journal homepage: http://civiljournal.semnan.ac.ir/

A Full Coupled Numerical Method for Dynamic Response of Metro Tunnel Subjected to Surface Explosion

Seyed Mohammad Hossein Khatami[1*], Hamed MomenAbadi[2]
1. Department of Civil Engineering, Technical and Vocational University (TVU), Tehran, Iran
2. M.Sc. Graduated, Department of Civil Engineering, Semnan University, Semnan, Iran
Corresponding author: *mkhatami@tvu.ac.ir*

ARTICLE INFO

Article history:
Received: 20 April 2021
Revised: 20 July 2021
Accepted: 13 September 2021

Keywords:
Surface explosion;
Metro tunnel;
ALE method;
LS-DYNA.

ABSTRACT

Terrorist explosion attacks have increased in recent years. Hand bombs are one of the means for terrorist operations because of their dangerous progressive damages. In this paper, a full coupled numerical method is adopted to study the dynamic response of a metro tunnel in the sandy loam. The numerical model is developed using LS-DYNA and will be able to present a realistic behavior for the physics of this phenomenon. In the current study, the ALE method has been used. The air, explosive charge, and soil are considered as ALE's parts; while, the structure of the tunnel has Lagrangian mesh. Two paths have been studied in the longitudinal and the circular directions for assessing tunnel lining safety. In the free-field state, the accuracy of the model is verified by comparing the peak pressure and acceleration in the soil with the empirical predictions available in the literature. The safety assessment has been done according to explosion vibration criteria. The tunnel would not be safe, as per the PPV standard, under the condition of w=500kg and R=4m. Tunnel crowns are the most vulnerable areas while the peak particle velocity is 19cm/s with maximum permanent vertical deformation.

1. Introduction

Terrorist blast attacks have increased in recent years. Hand bombs are one of the means for terrorist operations because of their dangerous progressive damages. For instance, World Trade Center in New York-2001, Madrid-Spain-2004, Moscow-Russia-2010, and the recent subway station incident in VolgogradRussia-2013 have caused human losses and significant building damages, especially in the railway transportation systems like underground metro tunnels.

How to cite this article:
Khatami, S., Momenabadi, H. (2022). A Full Coupled Numerical Method for Dynamic Response of Metro Tunnel Subjected to Surface Explosion. Journal of Rehabilitation in Civil Engineering, 10(3), 21-36.
https://doi.org/10.22075/jrce.2021.23198.1501

Researchers carried out extensive research on the dynamic response of masonry structures subjected to blast loading [1, 2].

The LCS analytical model is used to control the response of blast load acting on SDOF system is studied , the response of displacment is 50% is reduced in all the thress cases of loading, where as velocity 45% is reduced and accleration is 48% is reduced. [3]

Various numerical methods are used in order to study the response of buried concrete structures under the blast load. These methods are classified according to whether they are coupled or uncoupled. In the uncoupled system, the problem's physical process is divided into several consecutive steps. Each step's result is considered as the input for the previous step.

In this system, firstly, the history of free field stresses is measured, and then it is applied to the structure as boundary conditions. In this situation, the interaction between soil and structure hasn't been taken into consideration realistically. Various numerical analyses [4, 5] have been done on this basis. Yang [4] obtained the shock response spectra and compared them with SDOF analysis using ABAQUS explicit code.

In the full coupled numerical method, all the above steps are taken into consideration in one model. Up to now, because of the complexity of the problem's solution, fewer numerical studies have been allocated to this method. For instance, Wang et al. [6] modelled the soil adjacent to the explosive charge with the SPH method using AUTODYN hydro-code and also modelled the soil far from the blast zone with the FEM. Bartoli et al. [7] proposed a Bayesian method for the FEM updating of the masonry towers taking advantage of experimental data.

To model structures under blast loading, apart from LS-DYNA [8], ABAQUS/Explicit finite element code has made its presence known as a specialized tool with reliable performance [9].

Jayasinghe et al. [10, 11] studied the dynamic response of an aluminum and reinforced concrete pile in saturated sand under the effect of the subsurface blast with the Arbitrary Lagrangian-Eulerian (ALE) method with LS -DYNA hydro-code and calibrated the numerical results of peak pressure in the soil and horizontal displacement of the pile with the experimental data. Furthermore, De [12] analyzed the effect of the explosion over dry, cohesionless soil using the previous method. Crater size and strains at different locations of the underground structure were found to closely match those from other analyses and tests. Another developed method is a combination of the finite difference method (FDM) and the finite element method (FEM). [13].

In this approach, the soil is modelled using the FDM, which is suitable for the analysis of shock wave propagation in the nonlinear continuous zone, but the structure is analyzed using the FEM. Blast load is still in the term of stress or pressure.

It should be noticed that in an uncoupled model, analysis of the shock wave's effect on structure (especially structures with complicated geometry), wave reflection, and ground vibrations are simulated difficultly. The interaction between soil and structure, including slippage, separation, rebound, and

etc. are significant factors, which affect the structure's dynamic response [14].

Ma et al. [15, 16] studied soil-structure interaction due to subsurface blast. They numerically obtained modal and structural responses under the excitation of different dominant frequencies (10 –300 Hz) using a five-story plane frame structure. They developed an integrated analytical model for the prediction of the in-structure shock at blast loading and a free vibration phase. With the development of centrifuge scale tests [17, 18], studies on the blast damage assessment of underground structures have more improvements. Unfortunately, fewer studies have regarded the explosion in the railway transportation system, and it's necessary to study the hazards and losses of this incident for safety precaution.

The development of the full coupled numerical analysis will be an important step forward for designers of sensitive underground structures like metro tunnels.

Thai et al. [19,20] investigated the retrofitting of RC square columns exposed to blast loading by employing steel sheets and LS-DYNA [19,20].

The Finite Element Model Updating (FEMU) was used by Malekshahi and Akhaveissy [21] in order to calculate the maximum free-field pressure.

The comparison of the numerical analysis results in FEMU to field data shows a good consistency between the numerical results and the field data.

Mollaei et al. [22] studied different explosive behaviors of the circular and square RC columns. Results showed that the circular columns perform better under the sudden lateral pressure than equivalent square ones.

Kiran and Kori studied The effect of blast load on ten story structure. They reported that The response of a structural system exposed to blast load is 40% is reduced by using cladding material. [23]

In this paper, the dynamic response of a metro tunnel subjected to surface blast load is observed by the full coupled numerical method using LS - DYNA. At first, the free-field state and shock wave propagation in the soil is discussed. Then the concrete tunnel lining is analyzed, and the safety assessment is presented. The numerical results have been validated using the US Army Corps of Engineers TM5-855-1 manual [24].

2. Crater formation

Shock waves create the crater by highly compressing the soil adjacent to the explosive charge. The process of crater forming is complicated. Because of much of the blast energy dissipates in the air, various kinds of the crater will appeared. Figure 1 shows the schematic of a crater, rupture and plastic zones. Fiserova [25] and Luccioni [26] studied crater size at sub-surface blast situations. Fewer studies have been done for the crater size of the surface blast. The following equation is suggested without the consideration of soil properties:

$$D_r(m) = 0.8W^{\frac{1}{3}}(kg) \quad (1)$$

Where D_r is the true crater diameter and W is the weight of the explosive charge.

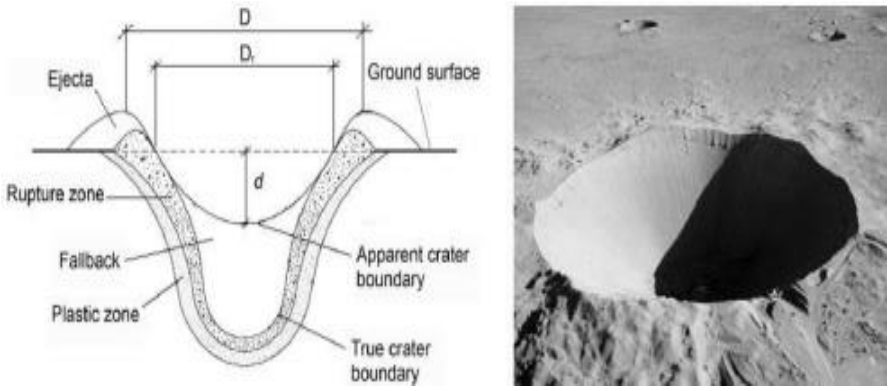

Fig. 1. Crater formation [25, 26].

3. Numerical modeling

In this section, a numerical model is introduced to analyze the damage of a metro tunnel in the soil affected by surface detonation, using the explicit nonlinear dynamic solver LS-DYNA. The finite element model consists of Air, TNT charge, soil, and tunnel lining. All the geometrical dimensions are shown in Figure 2, which has a similarity to Yang's model.[27] The cylindrical explosive charge is located in the middle point over the tunnel (critical destructive condition) at the interface between air and soil. The explosive charge weight and tunnel depth vary from 500 - 1000kg and 4 -10m, respectively.

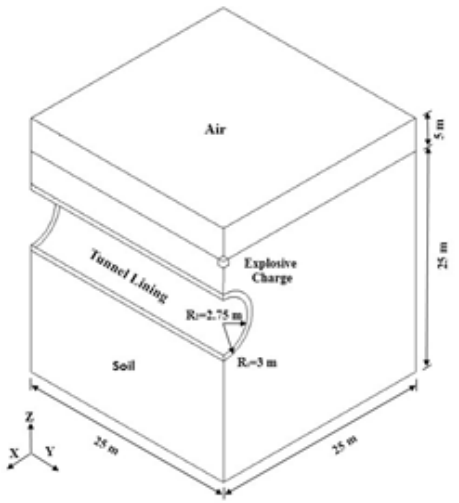

Fig. 2. Configuration of the numerical model.

3.1. The implemented numerical method

In the current study, the ALE method has been used. The air, explosive charge, and soil are considered as ALE's parts; while, the structure of the tunnel has Lagrangian mesh. It has to be mentioned that in the Lagrangian viewpoint, the mesh is aligned with the material. When a high distortion of mesh occurs, the elements' edges cross each other. As a result, the matrix Jacobian of the element's mapping will be negative. This issue will cause the loss of quality of the element and the inaccurate numerical result. In the Eulerian viewpoint, the material's mesh in the analysis zone is fixed in space, and the material moves through it. For this reason, this method does not have the limitation of large deformations, but it has a large defect in the prediction of material boundaries. In the ALE approach, which is based on a unique continuum mechanic's formula, whenever the deformation of Lagrangian elements is more than a level, the material in the elements is relocated using Eulerian method, and the new Lagrangian mesh is formed in accordance with the new location of the material. Therefore, for greater deformations, the unique capability of the Eulerian method could be used, and also the boundary of materials could be predicted with appropriate accuracy.

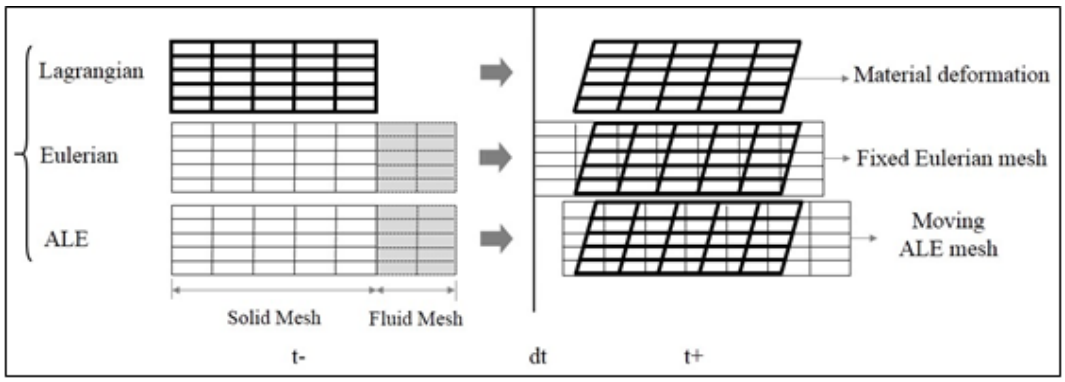

Fig. 3. Comparison of the Lagrangian, Eulerian and ALE methods [13].

The distinction of these methods is shown in Figure 3.

The*CONSTRAINED_LAGRANGE_IN_SOLID contact option in LS-DYNA is employed to model the soil-structure interaction. In order to reduce the computer calculation time, a symmetrical geometrical model is analyzed. The details of the finite element model are given in Table 1. and Figure 4. In the meshing process for air—explosive charge and soil parts—it has been tried that their interface nodes align with each other. In the consequent steps, these ALE's parts are merged, which is one of the most common ways of ALE contact. The convergence test is carried out by halving the mesh size in the analysis. It shows that the simulation converged when the mesh size is 25 cm. The air's upper face is free in all directions. In symmetric planes (YOZ and XOZ), displacement in normal directions is fixed in space. Moreover, on the lower and two other side surfaces, the Non-Reflecting boundary condition is applied.

Table 1. Detail of finite element model.

Part	Element type	Number of element	Average element size	Element formulation
Air	Solid ALE	25000	50 cm	ELFORM 11: 1 point ALE multi-material element
Explosive charge	Solid ALE	195	5 cm	ELFORM 11: 1 point ALE multi-material element
Tunnel lining	Solid	7200	20 cm	ELFORM 11: constant stress solid element
Soil	Solid ALE	132497	50 cm	ELFORM 11: 1 point ALE multi-material element

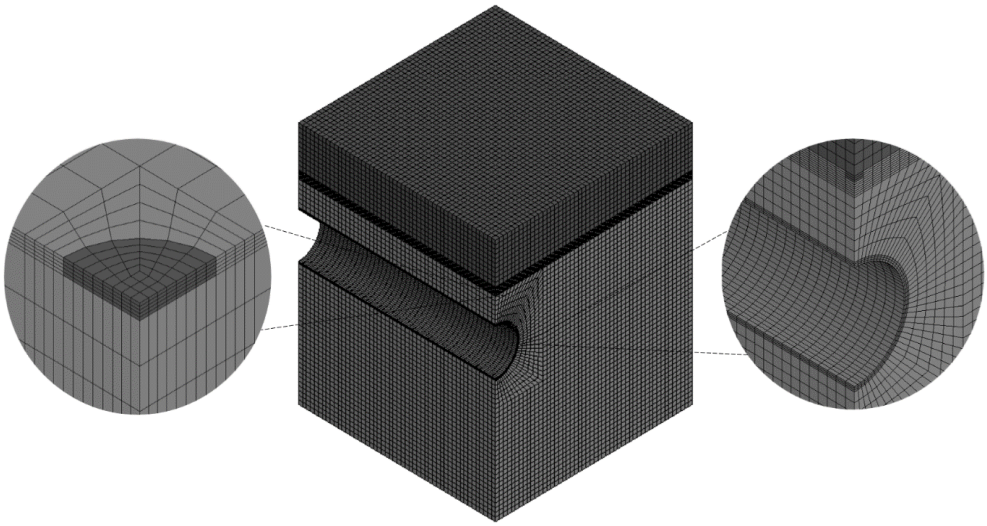

Fig. 4. Finite element mode.

3.2. Material models and equation of states

Materials' models assigned to air and explosion charge require an equation of states (EOS). It has to be noticed that SOLID elements in some materials' models are likely to increase density under compressive deformation. Therefore, EOS, a relationship between the pressures and density, is needed.

3.2.1. Air

The air layer is modeled by MAT 009_NULL with EOS known as LINEAR _POYNOMIAL: [28]

$$p = C_0 + C_1\mu + C_2\mu^2 + C_3\mu^3 + (C_4 + C_5\mu + C_6\mu^2)E_0 \quad (2)$$

Where $\mu = \frac{\rho}{\rho_0} - 1$ and P is the pressure, ρ and ρ_0 are current and nominal density, respectively. E_0 is initial internal energy per unit volume, and $C_0 - C_6$ are constants. Table 2 gives the parameters of the air model.

Table 2. Material properties of air [29].

$\rho(\frac{gr}{cm^3})$	$\rho_0(\frac{gr}{cm^3})$	C_0	C_1	C_2	C_3	C_4	C_5	C_6	$E_0(\frac{J}{m^3})$
1.29e-3	1e-3	0	0	0	0	0.4	0.4	0	2.5e5

3.2.2. Explosive charge

Explosive charge has been defined with MAT 008_HIGH_EXPLOSIVE_BURN and EOS JWL. This model is widely used in blast simulation as follows: [28]

$$p = A(1 - \frac{\omega\rho}{R_1})e^{-R_1\frac{\rho_0}{\rho}} + B(1 - \frac{\omega\rho}{R_1\rho_0})e^{-R_2\frac{\rho_0}{\rho}} + \frac{\omega\rho^2}{\rho_0}E_0 \quad (3)$$

Where A, B, R_1, R_2, and ω are material's constants, which are obtained from experimental tests. Explosive's density is

indicated by ρ_0. ρ is blast products' density, and E_0 is the initial energy per mass unit. Here, the TNT explosive charge has been selected, and its parameter has been listed in Table 3.

Table 3. Material properties of TNT explosive charge [18].

$\rho(\frac{gr}{cm^3})$	$\upsilon_D(\frac{m}{s})$	$P_{CJ}(MPa)$	$A(MPa)$	$B(MPa)$	R_1	R_2	ω	$\frac{\rho}{\rho_0}$	E_0
1.63	6930	2.1e4	3.73e5	3.7471e5	4.15	0.9	0.35	1	6e9

3.2.3. Soil

Soil type has been considered to be sandy loam, and the appropriate material model for it in LS-DYNA is MAT 005_SOIL_AND _FOAM which was presented by Krieg. This is a simplified model which at some occasions shows a behavior like a fluid). [28] Main parameters in this model include mass density ρ, shear modulus G, bulk modulus K_u on the unloading path, constant a_0 ، a_1 and a_2 which are related to pressure and yielding function P_{cut} for tensile failure. Table 4 and Figure 5 indicate relevant parameters corresponding to the Kulak. [30]

Table 4. Material properties of sandy loam. [30].

Parameter	Magnitude
RO	1.255
G	1.724
K	5.516
a_0, a_1, a_2	0, 0, 0.872
PC	0
VCR	0
EPS	Figure 5
P	Figure 5

The deviatory perfectly plastic yield function, ϕ, is described in terms of the second invariant J_2, pressure p and constants a_0, a_1, a_2 as:

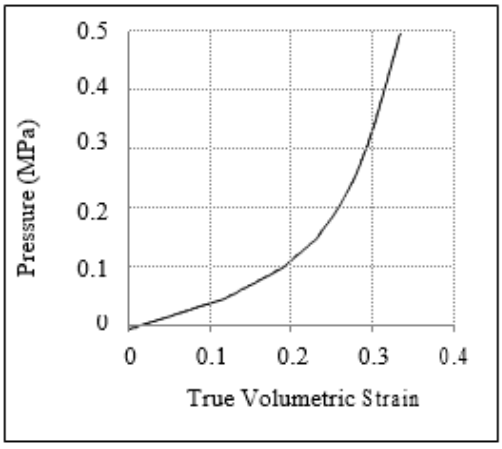

Fig. 5. Tri-axial hydrostatic pressure vs. volumetric strain for sandy loam [30].

$$\phi = J_2 - (a_0 + a_1 p + a_2 p^2) \quad (4)$$

On the yield surface $J_2 = \frac{1}{3}\sigma_y^2$ where σ_y is the uniaxial yield stress and there is no strain hardening on this surface as:

$$\sigma_y = (3(a_0 + a_1 p + a_2 p^2))^{\frac{1}{2}} \quad (5)$$

3.2.4. Tunnel Liner Structure

For concrete tunnel lining, MAT 003_PLASTIC_KINEMATIC has been used. This model is suited to model isotropic and kinematic hardening plasticity with the option of including rate effects. [28] Table 5 gives the parameters of the concrete tunnel model by the strength grade of the C50.

Table 5. Material properties of C50 for tunnel lining [27].

RO(gr/cm^3)	E(GPa)	PR	SIGY(MPa)	ETAN(MPa)	BETA	FS
Mass density	Yound's modulus	Poisson's ratio	Yield stress	Tangent modulus	Hardening parameter	Failure strain
2.65	39.1	0.25	100	4	0.5	0.8

4. Result and discussion

Since the initial hydrostatic pressures due to gravity are very small (by magnitude kPa) in comparison to the anticipated pressure of blast waves, the result is discussed in terms of dynamic response only. In the first simulation, shock wave in a free-field state (without tunnel structure) has been studied.

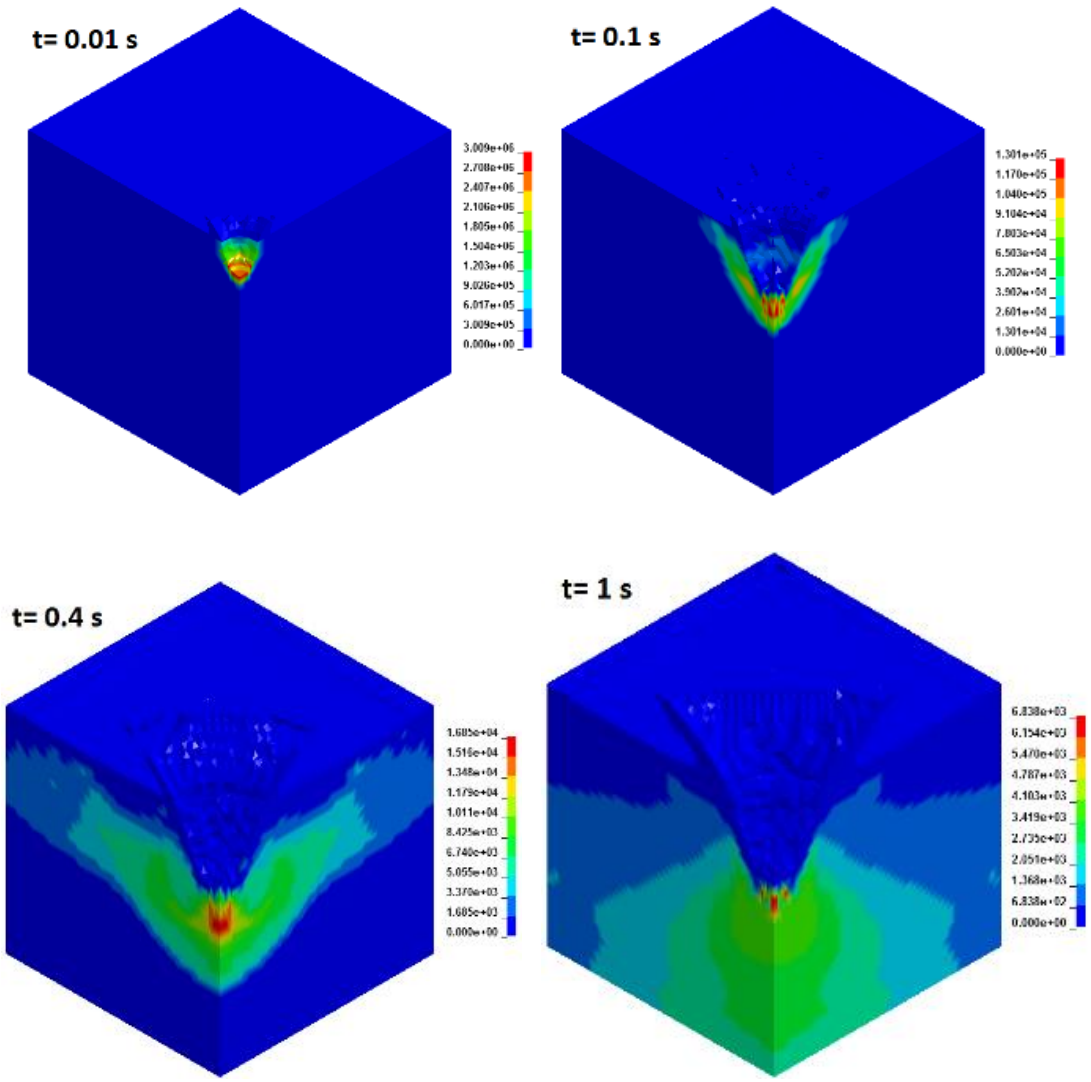

Fig. 6. Propagation of shock wave pressure in soil (free field).

Figure 6 shows pressure shock wave propagation in the soil until 0.2s for the first calculation case with 250 kg of explosive charge. The pressure waves propagate as semi-spherical shape, and the wavefront becomes larger. According to Figure 7, the stable crater has formed at t = 0.4s, with the true diameter and depth of $R_r = 5\ m$ and $D = 6.15$ m, respectively. By equation (2), $R_r = \frac{D_r}{2} = 4$ m, it is to be noticed that this difference is due to that this proposed equation does not consider soil property for blast analysis. For $t > 0.4\ s$ peak pressure of the compressive waves has attenuated and is reached to 6.8 kPa.

4.1. Verification of shock wave parameters

Up to now, some relationships for the determination of shock wave's parameters have been presented. The military manual [19] has been widely used in studies. [6], [14], [27] The following equations have been presented for estimation of peak pressure and peak acceleration, respectively:

$$p_p = 0.407\, f\, \rho_c \left(\frac{R}{W^{\frac{1}{3}}}\right)^{-n} \quad (6)$$

$$a_p = \frac{39.8\, fc}{W^{\frac{1}{3}}} \left(\frac{R}{W\frac{1}{3}}\right)^{-(n+1)} \quad (7)$$

Where P_p and a_p represent the peak pressure and peak acceleration, respectively. additionally, f is the coupling factor, d is the depth of the center of the charge, ρ_c is acoustic impedance, c is seismic velocity, R is the distance from the source, W is charge mass, and n is the attenuation coefficient. Figure 8 shows the diagram of the coupling factor versus a scale number of the blast ($\frac{d}{w^{\frac{1}{3}}}$) which for surface blast f ≈ 0.41.

In Figure9 and Figure 10, obtained numerical values for peak pressure and peak acceleration, respectively, are compared with predicted values. Straight lines express equations (6) and (7), and the triple-dot shows the best fit for numerical values. As shown, numerical results for peak acceleration have a good agreement with predicted values; however, the peak pressures are less than predicted values.

The proportion of discrepancy between results has increased with depth increase ($R > 7\ m$). This is because, in the TM manual, it has been assumed that the depth of buried charge should be enough for the formation of a complete blast zone. In other words, coupling coefficient f should be close to 1, while, here, the depth of buried charge is nearly zero. The proportion of absorbed energy in the air and soil in surface blasts will nearly be 53% and 47%, respectively, i.e., half of the explosion energy dissipated in the air. [27] Therefore, it's natural that the numerical results are less than predicted values.

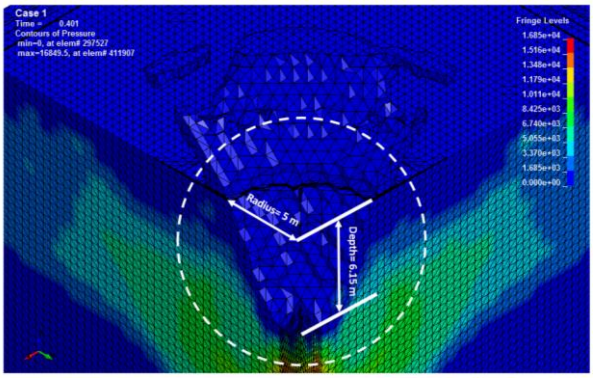

Fig. 7. Stable crater after 0.4s.

4.2. Dynamic response of tunnel

In this part, the effect of shock waves on the tunnel lining has been studied when the mass of the explosive charge and the tunnel depth are 500kg and 4m, respectively. By comparison with the free-field state, the tunnel prevents the propagation of shock waves in the more depth of the soil; in other words, the explosion energy transfers from the soil to the tunnel. Two target paths have been indicated in Figure 11 to assess the dynamic response of the tunnel. In path (a), five points from the section surface have been selected from different angles. Path (b) also included the horizontal distance of 0 to 25m from the center of the explosive charge.

According to the safety regulations for blasting, the safety criterion of blasting vibration velocity for traffic tunnel is 10 –20 cm/s. [31] Apart from that, the safety factor has been assumed 2 to 4 in order to satisfy the construct safety against the subsequent destruction. Therefore, the safe vibration limit of the tunnel is up to 5 cm/s. Figure 12 indicates the effective stress on the tunnel lining. The maximum effective stress has increased to 9.1 MPa at the time t=0.14s. The strength grade of the concrete is C50, the uniaxial compression strength of which is 23.1MPa [27].

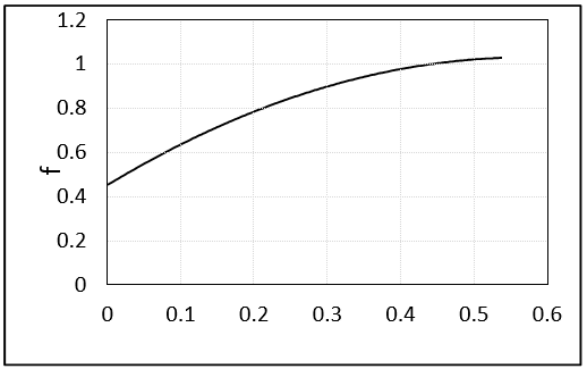

Fig. 8. Coupling factor vs. scaled distance.

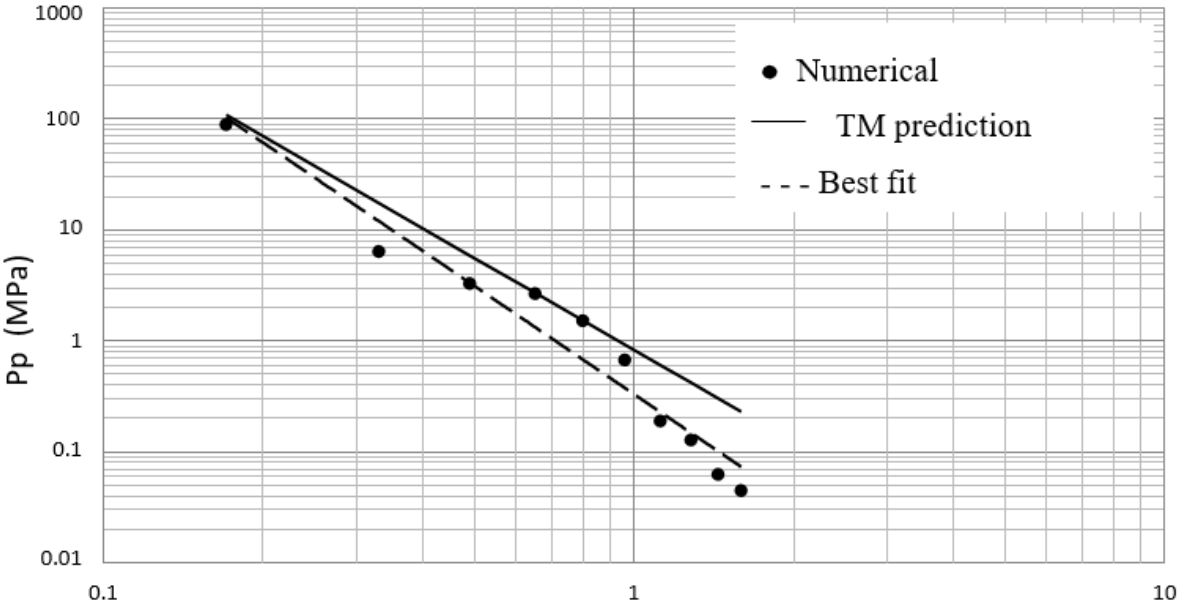

Fig. 9. Attenuation of the peak pressure in soil (free field).

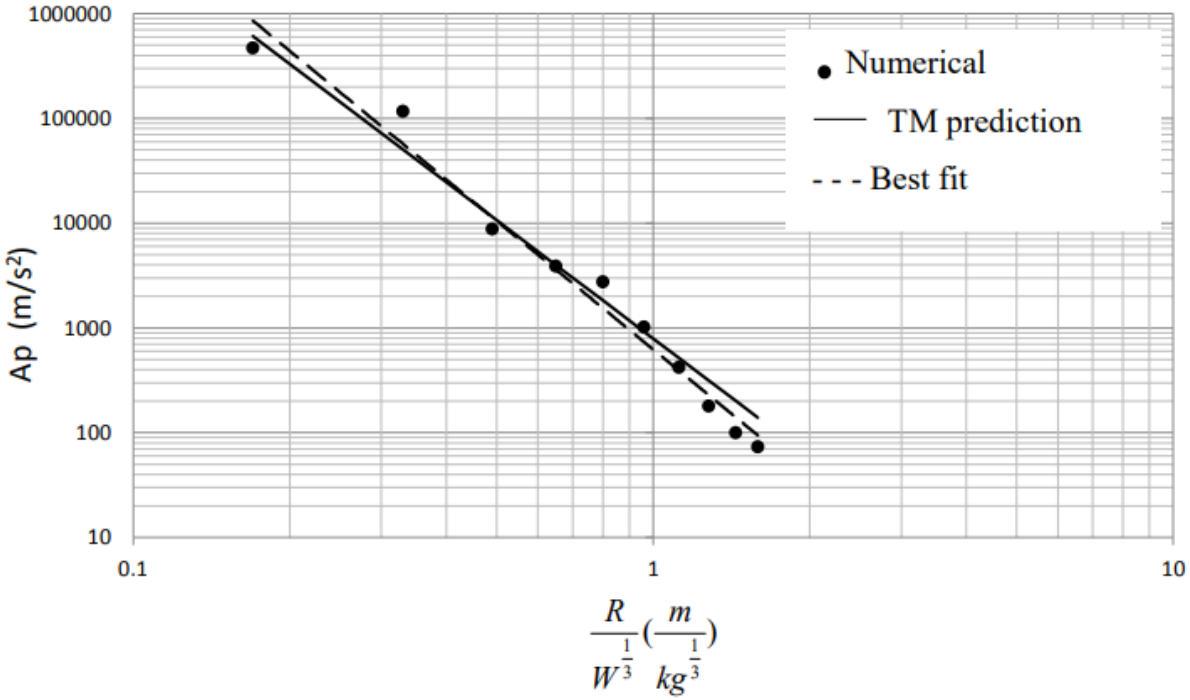

Fig. 10. Attenuation of the peak acceleration in soil (free field).

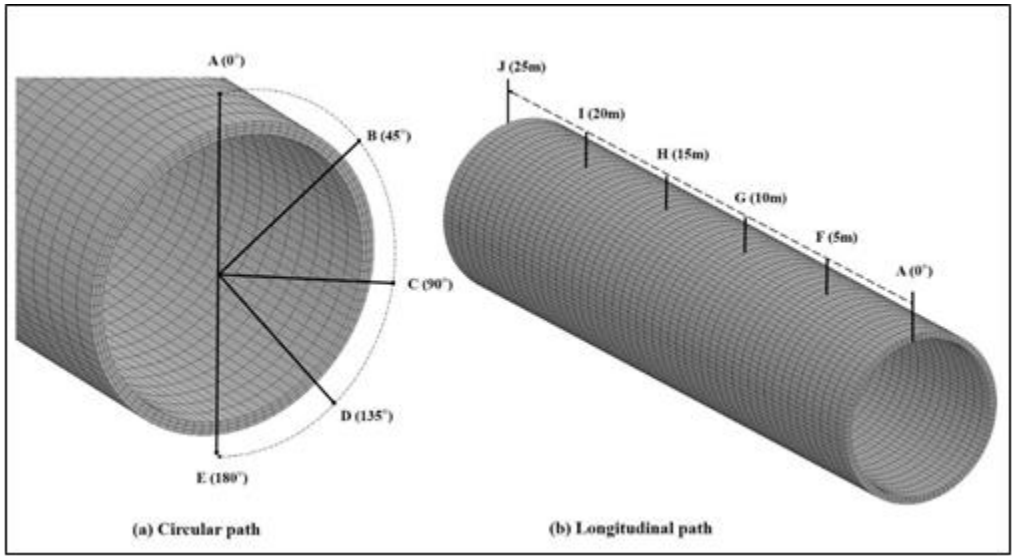

Fig. 11. Two paths on the tunnel lining.

According to the effective stress criteria of Von-Misses, although the imposed and implemented stress amount is less than the limit of ultimate strength, as seen in Figure 13 and 14, the vertical peak particle velocity (PPV) for the points, A and C are 18 cm/s and 20 cm/s, respectively. Therefore, the tunnel would not be safe in this condition.

Figure 15 shows the history of vertical acceleration related to the tunnel lining on point A that indicates the specification of high amplitude, short time, and fast authentication. Figures 16 and 17 indicate the vertical deformation for the target points from the circular and longitudinal paths.

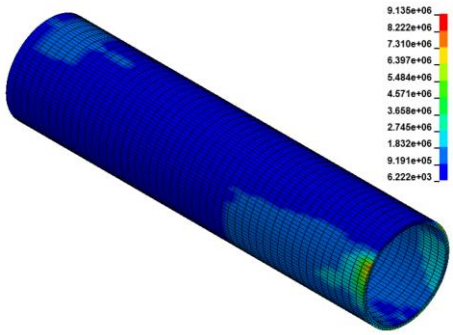

Fig.12. Effective stress of Von -Misses on the tunnel lining at t=0.14s.

The tunnel has sustained permanent deformation on some of the points that its maximum amount at point A on the Z and X directions are 9.1 cm and 1.89 cm, respectively. As shown in Figure 17, in the longitudinal path, the vertical deformation has happened from point A to point J with a 0.4 cm relative offset.

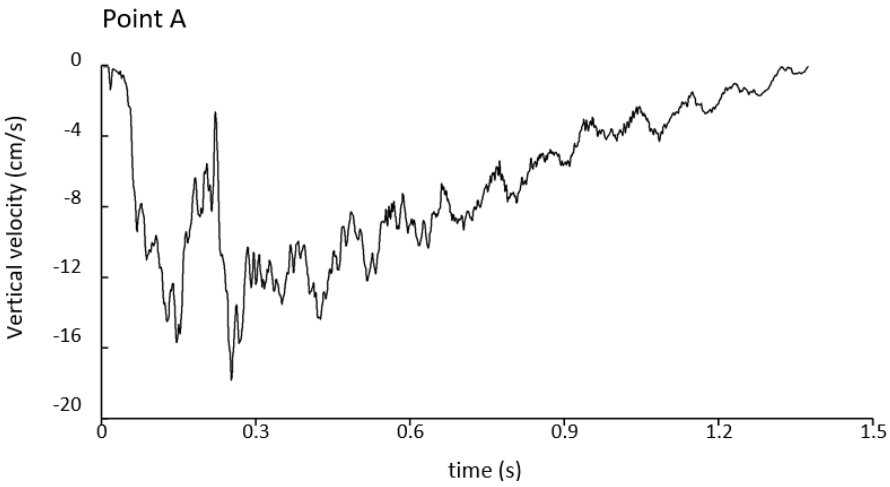

Fig. 13. Vertical velocity of points A.

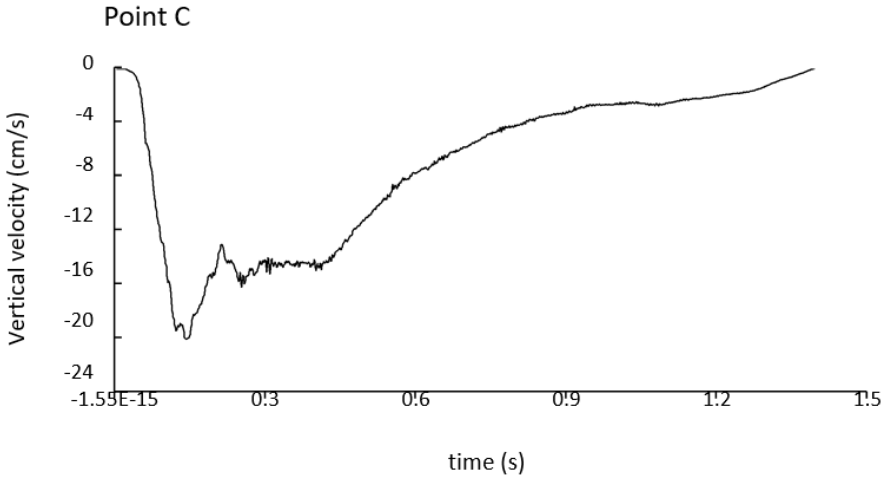

Fig. 14. Vertical velocity of points C.

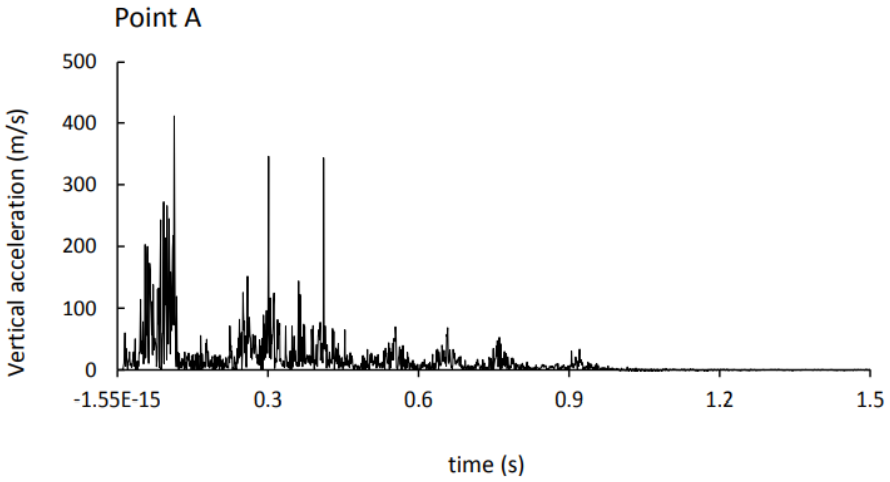

Fig. 15. Vertical acceleration of tunnel lining on point A.

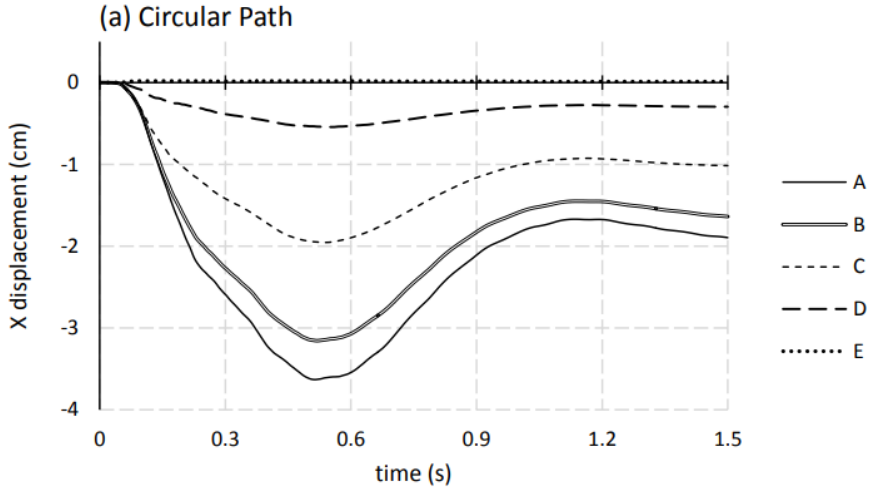

Fig. 16. Deformation of the tunnel lining (a) circular path.

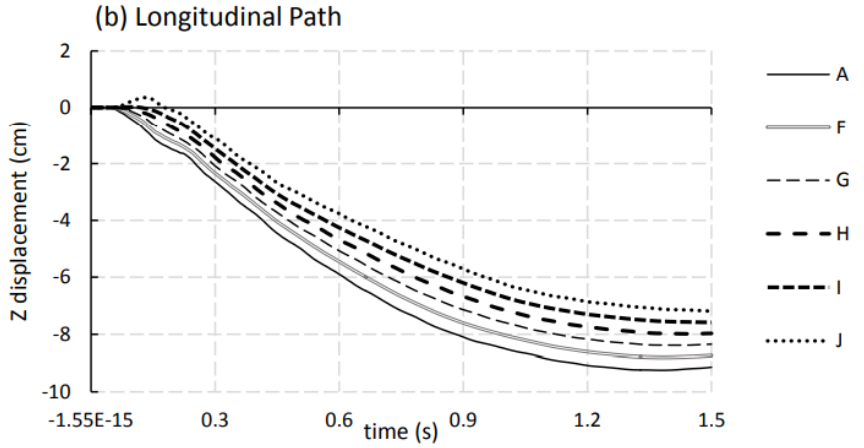

Fig. 17. Deformation of the tunnel lining (b) longitudinal path.

5. Conclusion

In this paper, the dynamic response of a metro tunnel subjected to the surface blast has been studied with the full coupled numerical method using LSDYNA. In the free-field state, the blast waves propagate in the soil by the semi-spherical shape. The accuracy of the numerical models for the peak pressure and acceleration are verified by the US military manual (TM5 -855 -1). Two paths have been studied in the longitudinal and the circular directions for assessing the tunnel lining safety.

- The tunnel will not be safe, as per the PPV standard, under the condition of w=500kg and R=4m.

-The maximum damage occurred at point A with a maximum permanent vertical deformation equal to 9.1cm with PPV=18cm/s.

-The maximum effective stress on the tunnel lining has increased to 9.1 MPa at the time t=0.14s.

- The history of vertical acceleration related to the tunnel lining on point A indicates that the specification of high amplitude, short time, and fast authentication

- The maximum X displacement occurs at point A in approximately 0.6 seconds

In the future, the effect of soil type and concrete strength grade on the dynamic response of the metro tunnel can be seen.

References

[1] Chen, L., Feng, Q., Fan, J. (2014). "Responses of masonry infill walls retrofitted with CFRP, steel wire mesh and laminated bars to blast loadings." Advances in Structural Engineering, 17(6), pp. 817-836.

[2] Chen, L., Hao, H., Fan, Q. (2013). "Calibration and discussion of parameters of Mat_72Rel3 constitutive model on clay brick and mortar materials." in Proceedings of 15th International Symposium on the Interaction of the Effects of Munitions with Structures.

[3] Kiran, K., Kori, J.G. (2018). "Controlling Blast Loading of the Structural System by Cladding Material." Computational Engineering and Physical Modeling,Vol. 1, pp. 79 -99.

https://doi.org/10.22115/cepm.2018.141294.1038

[4] Yang, Z. (1997). "Finite element simulation of response of buried shelters to blast loadings." Finite elements in analysis and design,Vol. 24, pp. 113 -132.

[5] Hinman, E. (1989). "Effect of deformation on the shock response of buried structures subject to explosions." Structures under shock and impact, Elsevier, pp. 455 -465.

[6] Wang, Z., Lu, Y., Hao, H., Chong, K. (2005). "A full coupled numerical analysis approach for buried structures subjected to subsurface blast." Computers & structures, Vol. 83, pp. 339 -356.

[7] Bartoli, G., Betti, M., Facchini, L., Marra, A., Monchetti, S. (2017). "Bayesian model updating of historic masonry towers through dynamic experimental data." Procedia engineering, Vol. 199, pp. 1258-1263.

[8] Livermore Software Technology Corporation. (2018). LS-DYNA R11 Keyword User's Manual.

[9] Akbarzadeh Bengar, H., Yavari, M. R. (2016). "Simulation of the Reactive Powder Concrete (RPC) Behavior Reinforcing with Resistant Fiber Subjected to Blast Load." Journal of Rehabilitation in Civil Engineering, Vol. 4(1), pp. 63-77.

[10] Jayasinghe, LB., Thambiratnam, DP., Perera, N., Jayasooriya, J. (2013).

"Computer simulation of underground blast response of pile in saturated soil." Computers & Structures, Vol. 120, pp. 86 - 95.

[11] Jayasinghe, LB., Thambiratnam, DP., Perera, N., Jayasooriya, J. (2014). "Blast response of reinforced concrete pile using fully coupled computer simulation techniques." Computers & Structures, Vol. 135, pp. 40 -49.

[12] De, A. (2012). "Numerical simulation of surface explosions over dry, cohesionless soil." Computers and Geotechnics, Vol. 43, pp. 72 - 79.

[13] Zimmerman, H., CG, Carney., J, Ito., Y, Cratering. (1990). "ground shock environment prediction of buried armor piercing bomb in dry Socorro plaster sand." Technical Report CRT-3295-010-01, California Research and Technology, Chatsworth Calif.

[14] Nagy, N., Mohamed, M., Boot., J. (2010). "Nonlinear numerical modelling for the effects of surface explosions on buried reinforced concrete structures." Geomechanics and Engineering, Vol. 2, pp. 1 -18.

[15] Ma, H., Quek, S., Ang, K. (2004). "Soil–structure interaction effect from blast-induced horizontal and vertical ground vibration." Engineering structures, Vol. 26, pp. 1661 -1675.

[16] Ma, G., Zhou, H., Lu, Y., Chong, K. (2010). "In - structure shock of underground structures: A theoretical approach." Engineering Structures, Vol. 32, pp. 3836 - 3844.

[17] De, A., Zimmie, TF., Abdoun, T., Tessari, A. (2010). "Physical modeling of explosive effects on tunnels." Fourth international symposium on tunnel safety and security, Frankfart am Main, Germany. pp. 159 -167.

[18] Simpson, P., Zimmie, T., Abdoun, T. (2006). "Explosion tests on embankment models in the geotechnical centrifuge." Proceedings of International Conference on New Developments in Geoenvironmental and Geotechnical Engineering.

[19] Thai, D. K., Pham, T. H., Nguyen, D. L. (2020). "Investigation on the Damage of RC Columns Covered by Steel Plate under Blast Loading." The Structural Design of Tall and Special Buildings, (in press).

[20] Thai, D. K., Pham, T. H., Nguyen, D. L. (2020). "Damage assessment of reinforced concrete columns retrofitted by steel jacket under blast loading. " The Structural Design of Tall and Special Buildings, Vol. 29(1), e1676.

[21] Malekshahi, M., Akhaveissy, A.H. (2020). "Experimental Study of Masonry Structure under Impact Loading and Comparing it with Numerical Modeling Results via Finite Element Model Updating." Journal of Rehabilitation in Civil Engineering, pp. 90-105.

[22] Mollaei, S., Babaei, M., Jalilkhani, M. (2021). "Assessment of Damage and Residual Load Capacity of the Normal and Retrofitted RC Columns against the Impact Loading." Journal of Rehabilitation in Civil Engineering, pp. 29-51.

[23] Kiran, K., Kori, J.G. (2019). "Blast Mitigations of Mid Rise Structures by Cladding Material." Computational Engineering and Physical Modeling,Vol. 2, pp. 78 -94.
https://doi.org/10.22115/cepm.2020.196935.1066

[24] Army USDot. (1986). "Fundamentals of protective design for conventional weapons." Headquarters, Department of the Army.

[25] Fiserova., D. (2006). "Numerical analysis of buried mine explosions with emphasis on effect of soil properties on loading." Cranfield University.

[26] Luccioni, B., Ambrosini, D., Nurick, G., Snyman, I. (2009). "Craters produced by

underground explosions." Computers & Structures, Vol. 87, pp. 1366 -1373.

[27] Yang, Y., Xie, X., Wang, R. (2010). "Numerical simulation of dynamic response of operating metro tunnel induced by ground explosion." Journal of rock mechanics and geotechnical engineering, Vol. 2, pp. 373-384.

[28] Hallquist, JO. (2007). "LS-DYNA keyword user's manual. Livermore Software Technology Corporation," Version 970.

[29] Cowler, M., Birnbaum, N. (1989). "AUTODYN user manual." Century Dynamics Inc, Oakland, (USA).

[30] Kulak, RF., Bojanowski, C. (2011). "Modeling of Cone Penetration Test Using SPH and MM -ALE Approaches." 8th European LS-DYNA® Users Conference.

[31] Jiang, N., Zhou, C. (2012). "Blasting vibration safety criterion for a tunnel liner structure." Tunnelling and Underground Space Technology, Vol. 32, pp. 52 -57.